

Temperature Profile Measurement of a Graphite Tube Furnace Using Optical Fibre and Platinum Thermocouples

Khaled Chahine^{*}, Mark Ballico^{*}, John Reizes^{**} and Jafar Madadnia^{**}

^{*}National Measurement Institute, Australia
P O Box 264, Lindfield, NSW 2070

^{**}University of Technology, Sydney

P O Box 123, Broadway, NSW 2007

Email: Khaled.Chahine@measurement.gov.au

Abstract

The surface temperature of the Thermogage blackbody graphite tube furnace used at the National Measurement Institute Australia, NMIA, for the calibration of pyrometers was measured using a silica optical fibre and Pt/Pt-Rh thermocouples. The silica optical fibre was bent using a H₂ flame causing some deformation to the bent area. This resulted in a light leakage from the deformed area, which was experimentally assessed. The optical fibre measurements were corrected from irradiances from other parts of the graphite tube using view factors obtained from the literature. These corrections were small and positive near the middle of the tube but large and negative nearer the end. A model for the uncertainty in the temperature corrections was also developed. The corrected optical fibre results were found to agree well with measurements made using Pt/Pt-Rh thermocouples. Further investigation is required to reduce systematic error in the thermocouple data.

1. Introduction

A 48kW Thermogage blackbody furnace is used as a primary radiance standard for the temperature calibrations of pyrometers up to 3000°C. At NMIA, the increasingly stringent uncertainty requirements from industry necessitate the improvement of the temperature uncertainty associated with using this blackbody. Presently, this uncertainty is approximately 2 °C at 2000 °C, which is mainly due to the emissivity of the blackbody. The emissivity was calculated to be 99.2% at a temperature of 1000 °C and a wavelength of 650 nm, increasing to 99.9% in some cases [1]. This leads to an uncertainty of 0.8% associated with the radiance of the Thermogage blackbody.

In order to improve the furnace temperature uncertainty and to allow its use as a standard source for ultra-violet radiation, the emissivity must be increased to 99.9% for all cases. The aim of this work is to achieve this increase by improving the temperature uniformity of the Thermogage blackbody furnace (Figure 1). Numerical heat transfer models are being developed to optimize the thermal design of the heater element and its insulation. To validate these models, precise heat balance and temperature profile measurements are required.

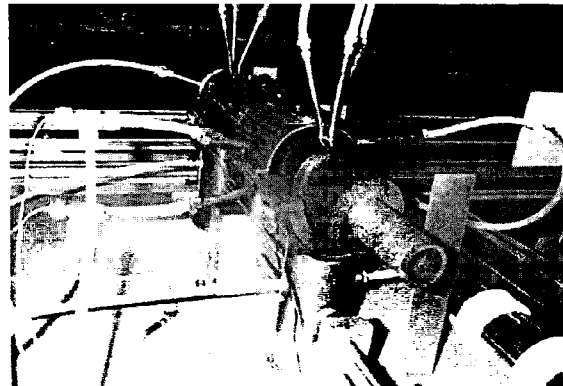


Figure 1. Thermogage 48kW blackbody furnace at the National Measurement Institute Australia.

Temperature profile data has previously been obtained using thermocouples, however the steep temperature profile in the furnace may result in significant systematic errors in these measurements. In this paper, we compare several different thermocouple measurements with a new method based on a silica optical fibre to assess the magnitude of these errors. A model for corrections and their uncertainties due to reflection of light within the furnace was developed and applied to the measurement data.

The good level of agreement between the two different measurement methods gives more confidence to the measured temperature profiles.

2. Pt/Pt-Rh Thermocouple Measurements

The first method of measuring the graphite tube surface temperature profile uses Pt/Pt-Rh thermocouples, shown in Figure 2. The platinum wires and the alumina tube have significant thermal conductivity and therefore, when placed in the very steep temperature gradients inside the furnace tube (over 100 °C/cm), will conduct heat away from the measurement point resulting in a lower measured temperature.

At higher temperatures, there is very significant radiated heat flux from the tube inner surface (mainly due to the cold parts of the tube). When the thermocouple is placed on the surface then it will, to some extent, act as a "blanket", reducing radiative surface losses and causing a higher measured temperature.

One method to investigate the magnitude of these two effects is to examine the difference between measurements made with different thermocouple insulators. In figures 6 and 7, results are presented for thermocouples with alumina tubes 3.2 and 4.2 mm in diameter respectively. The temperature of the graphite tube was measured from its centre to its end at 10 mm intervals.

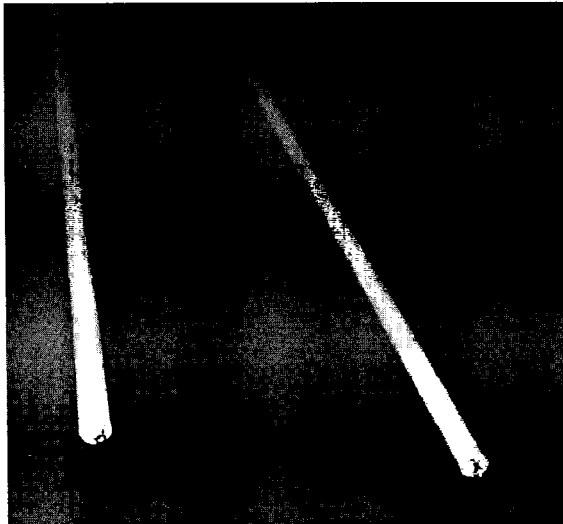


Figure 2. Pt/Pt-Rh thermocouple wires with 0.5 mm diameter inside alumina tubes with outside diameters of 4.2 and 3.2 mm.

The temperatures measured by the 3.2 mm diameter thermocouple are higher than the 4.2 mm thermocouple, with the differences becoming larger

at higher temperature gradients. This suggests that conduction effects dominate at 1000 °C (the temperature at which the blackbody was set for these experiments).

3. Optical Fibre Temperature Measurements

The graphite tube is 300 mm long and 25 mm in diameter and contains a wall septum in the middle, as shown in Figure 3. To view a measurement region with a spatial resolution of a few millimetres, most commercial pyrometers require F/20 to F/50 viewing optics (i.e. a viewing cone with an apex angle of 1-2°). Measuring the wall near to the centre of the furnace tube thus requires near tangential viewing. For graphite, the specular reflection component then becomes very significant, and will tend to merely reflect the temperature of the furnace septum. Other means had to be devised to collect light from the furnace wall surface for the pyrometer.

The solution to this problem was to bend a silica optical fibre to an angle of 45° to collect light from the graphite furnace tube surface. The cladding of the silica fibre was first removed, then using a H₂ flame the fibre was heated until it started to bend under its own weight. The fibre was removed from the heat source once the bend angle reached around 45°. Removal of the cladding and deformation introduced around the bend and the heated area may result in light leakage from the fibre. This leakage had to be investigated and the measurement uncertainty caused by this leakage had to be quantified at a wavelength of 850 nm, the operating wavelength of the pyrometer.

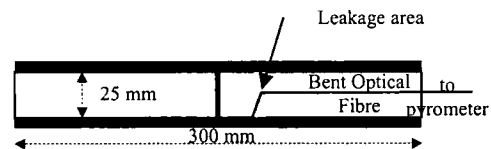


Figure 3. Schematic diagram of the graphite tube with dimensions.

The bent silica fibre was connected to a multimode fibre, the end of which was viewed by the NMIA pyrometer MTSP, which has F/10 optics and a 1 mm target spot. The detector signal V_m was converted to a temperature using Planck's law,

$$V_m \propto E = \frac{2\pi C_1}{\lambda^5 (e^{C_2/\lambda T} - 1)} \quad (1)$$

where E is the energy, C_1 and C_2 are the first and second Planck's constants, λ is the wavelength and T

is the absolute temperature. The pyrometer used had a 10 nm bandwidth filter at 850 nm. The MTSP has a voltage output V_m varying from ~10 V at 1000 °C to less than 0.05 V below 500°C. For a fixed wavelength λ of 850 nm the value of $C_2/\lambda T \gg 1$, therefore the calibration equation given in (1) becomes

$$V_m = V_o e^{-C_2/\lambda T} \quad (2)$$

where V_o is a constant. This constant can be determined by calibrating the pyrometer against a thermocouple reading in an isothermal environment. This calibration method automatically includes any fibre coupling or transmission losses. In our situation, the optical fibre was placed in the middle of the graphite tube and then V_o was calculated from the measured voltage and the value of the absolute temperature which was measured by a thermocouple.

The leakage from the bent area was measured using the experimental setup in shown Figure 4. Light from a tungsten halogen (QTH) lamp was collimated, filtered by an 850 nm interference filter, and focussed into a 1 mm multimode fibre by a fibre coupler. This was coupled to the bent silica fibre, the end of which was placed inside a 100 mm integrating sphere. An HP3458A multimeter measured the photocurrent of a silicon photodiode mounted on the sphere.

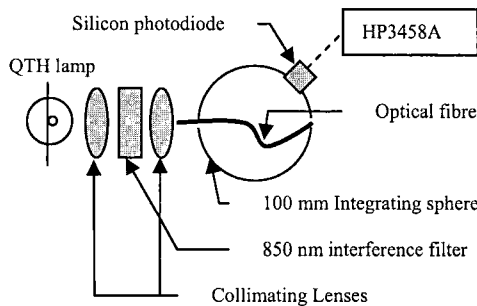


Figure 4. Schematic diagram of the leakage testing setup.

The total optical power E , launched into the fibre was assessed by placing it wholly inside the integrating sphere. The power leaking from the bent area, ΔE , was measured by carefully aligning the fibre tip, so that light directly radiated from the tip escaped through a small hole in an aperture placed in the sphere wall. A ratio of $\Delta E/E = 7.3\%$ was measured. Although the measured leakage is relatively large, the contribution of this leakage to the total temperature uncertainty is minimised by the fact that the bent area where the leakage occurred, shown in Figure 3, is almost on the top of the fibre tip where measurement occurs. Any leakage from

and to the fibre is mainly due to the radiation from and to the measured area. The leakage to other areas of the tube should not be more than 10% of the leakage, or $\Delta E/E = 0.73\%$.

For a narrow bandwidth optical pyrometer, equation (3) was used to calculate the error in temperature ΔT arising from an error in measured optical signal [2],

$$\frac{\Delta T}{T} = \frac{\lambda T}{c_2} \frac{\Delta E}{E} \quad (3)$$

Using this equation, the uncertainty in temperature for our measurements was calculated to be no more than 0.05% or 0.7 °C at 1000 °C and therefore could be ignored.

4. Silica Optical Fibre Corrections

Measurements of the temperature profile of the graphite tube were conducted using the bent optical fibre. The furnace temperature was set at a temperature of 1000 °C. Similarly to the thermocouple measurements, the surface temperature of the graphite tube was measured from the centre of the graphite tube to its end at different positions, i , at distances 10 mm apart.

For our work, the only temperature measurements of interest are within 120 mm from the centre as this is the area of the tube mostly affecting the centre wall emissivity. In addition, the measurements at low temperatures have large uncertainties due to the small signal and large reflections.

The radiant exitance measured by the pyrometer at a position i consists of the radiant exitance due to the thermal radiation arising from the surface temperature and the irradiances reflected from other places inside the graphite tube. This can be expressed as

$$M_i = \varepsilon M_{p(T),i} + (1 - \varepsilon) E_i \quad (4)$$

where M_i is the radiant exitance measured by the pyrometer at i , ε is the emissivity of graphite, $M_{p(T),i}$ is the radiant exitance due to the surface temperature, and E_i is the total irradiance from other surfaces inside the graphite tube onto i . Rearranging equation (4) and solving for $M_{p(T),i}$ gives

$$M_{p(T),i} = \frac{M_i}{\varepsilon} - \frac{(1 - \varepsilon)}{\varepsilon} E_i \quad (5)$$

which can be used to calculate the radiant exitances due to surface heat and then convert them into temperature readings using Planck's radiation law.

To simplify the computation of E_i , the graphite tube was assumed to be divided into ring elements with 10 mm width, this being the distance between measured positions. The total irradiance E_i on one ring element consists of the other ring elements' irradiances and the irradiance from the middle wall inside the graphite tube (refer to Figure 3). This is given by the following equation

$$E_i = \sum_{j=0}^n M_{j,r} F_{ji} \frac{A_j}{A_i} + M_{i,w} F_{wi} \frac{A_w}{A_i} \quad (6)$$

Combining equations (3) and (4) gives

$$M_{p(T),i} = \frac{M_i}{\varepsilon} - \frac{(1-\varepsilon)}{\varepsilon} \left[\sum_{j=0}^n M_j F_{ji} \frac{A_j}{A_i} + M_w F_{wi} \frac{A_w}{A_i} \right] \quad (7)$$

where n is the number of rings, M_j and M_i are the radiant exitances from other rings and the middle wall respectively, F_{ji} and F_{wi} are the view factors with the configurations of two ring elements and wall ring element respectively, A_i and A_j are the areas of the ring elements, and A_w is the wall area. Schematic diagrams of these two view factor configurations are shown in Figure 5.

Equations for the view factors were obtained from [3, pp.848] to be

$$F_{ji} = \left[1 - \frac{2X^3 + 3X}{2(X^2 + 1)^{3/2}} \right] dX_i \quad (8.a)$$

$$F_{wi} = \frac{X^2 + \frac{1}{2}}{\sqrt{X^2 + 1}} - X \quad (8.b)$$

$$X = \frac{x}{2r} \quad (8.c)$$

The radiant exitance $M_{p(T),i}$ at each position along the tube was calculated using equations (7) and (8.a-c). To simplify these calculations, all surfaces were assumed to follow Lambert's cosine law which make them independent of their viewing angle, and due to the high emissivity of graphite (0.85) only first order reflections were taken into consideration. Values for $M_{p(T),i}$ at each node i due only to the surface

temperature were calculated and then converted into temperatures (refer to section 3).

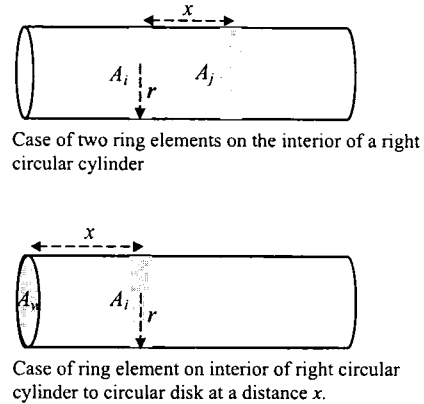


Figure 5. Schematic diagram of two view factor configurations.

5. Uncertainty in Reflection Corrections

The uncertainty in $M_{p(T),i}$ consists of the uncertainties u_ε , u_{M_i} , u_{M_w} and u_{M_j} in the emissivity ε and the measured signals M_i , M_w and M_j respectively. The uncertainties due to the view factors and areas are small and therefore were ignored. The uncertainties of the measured signals u_{M_i} , u_{M_w} and u_{M_j} were obtained from the standard deviations of the pyrometer readouts and found to be about 1.4% each. According to [4], the total uncertainty $u_{M_{p(T),i}}$ is calculated using the following equation

$$u_{M_{p(T),i}} = \left[(c_\varepsilon u_\varepsilon)^2 + (c_{M_i} u_{M_i})^2 + (c_{M_w} u_{M_w})^2 + \sum_{\substack{j=0 \\ j \neq i}}^n (c_{M_j} u_{M_j})^2 \right]^{1/2} \quad (9)$$

where $u_{M_i} = u_{M_j} = u_{M_w} = 1.4\%$ of the measured signal, and c_ε , c_{M_i} , c_{M_w} and c_{M_j} are the sensitivity factors given by the following partial differential equations

$$c_\varepsilon = \frac{\delta M_{p(T),i}}{\delta \varepsilon} = \frac{1}{\varepsilon^2} \left[-M_i + M_w F_{wi} \frac{A_w}{A_i} + \sum_{\substack{j=0 \\ j \neq i}}^n \left(M_j F_{ji} \frac{A_j}{A_i} \right) \right] \quad (10.a)$$

$$c_{M_i} = \frac{\delta M_{p(T),i}}{\delta M_i} = \frac{1 - F_{ii} + \epsilon F_{ii}}{\epsilon} \quad (10.b)$$

$$c_{M_w} = \frac{\delta M_{p(T),i}}{\delta M_w} = -\frac{1 - \epsilon}{\epsilon} F_{wi} \frac{A_w}{A_i} \quad (10.c)$$

$$c_{M_j} = \frac{\delta M_{p(T),i}}{\delta M_j} = -\frac{1 - \epsilon}{\epsilon} F_{ji} \frac{A_j}{A_i} \quad (10.d)$$

The value in equation (10.d) is only for one value of j . On the other hand, the summation in equation (9) is for all values of j from 0 to n except when $j = i$.

The uncertainty in the temperatures can be obtained using equation (3).

6. Results

Figure 6 shows plots of the optical fibre measurements, the corrected optical fibre measurements with the calculated uncertainty, and the Pt/Pt-Rh thermocouple measurements using two different alumina tubes. Figure 7 shows the same data on an expanded scale.

The reflection corrections to the optical fibre measurements are small within 80 mm from the centre of the tube, due to the near isothermal conditions in this area. The corrections become larger in the cooler regions, where the radiated optical power is very small compared to the reflections from the hotter (central) area of the graphite tube. For example the blackbody radiance at 850 nm is 50 times larger at 1000 °C than at 700 °C.

For the use of the Thermogage furnace as a blackbody source, it is the temperature region within a few diameters of the blackbody cavity end that is of most importance (within 50 mm of the centre of the tube). In this region, the measurements from the corrected fibre and two thermocouples all show a temperature difference of about 35 °C (within a range ± 1.5 °C). This gives us greater confidence in the measured gradient. Previously, only one set of data was available, and it was not clear if the measured gradient was real or an artefact of systematic errors in the thermocouple data.

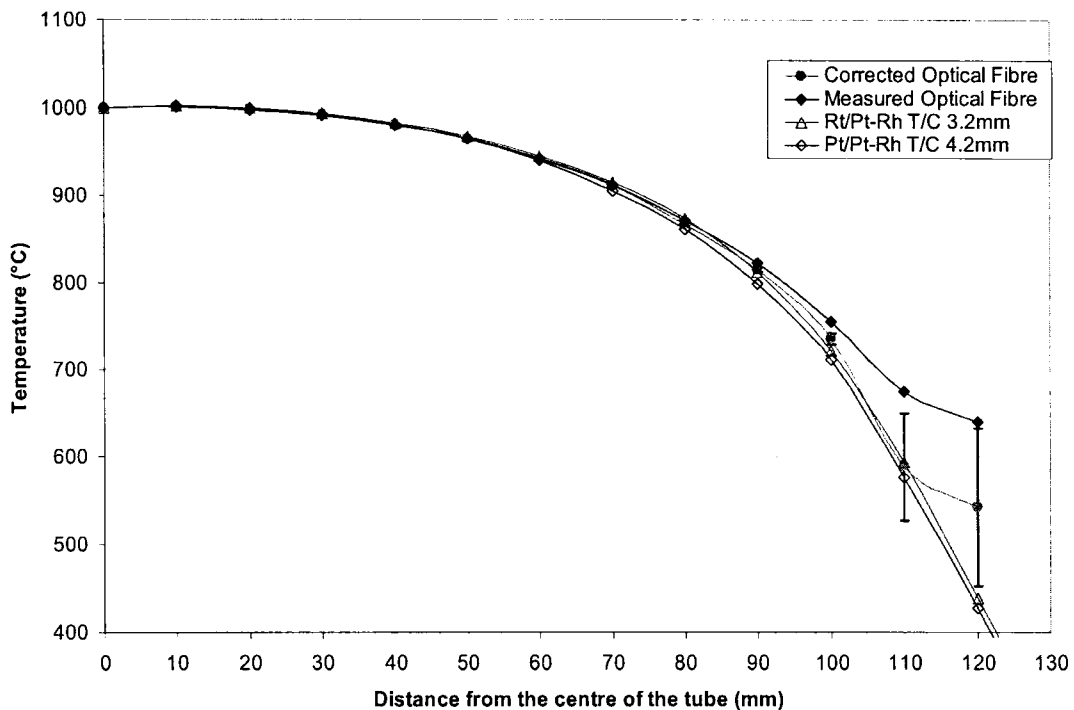


Figure 6. Plot of the optical fibre measured and corrected results with their uncertainty bars compared with the measurements taken by Pt/Pt-Rh thermocouple wires in alumina tubes with 3.2 and 4.2 mm diameter.

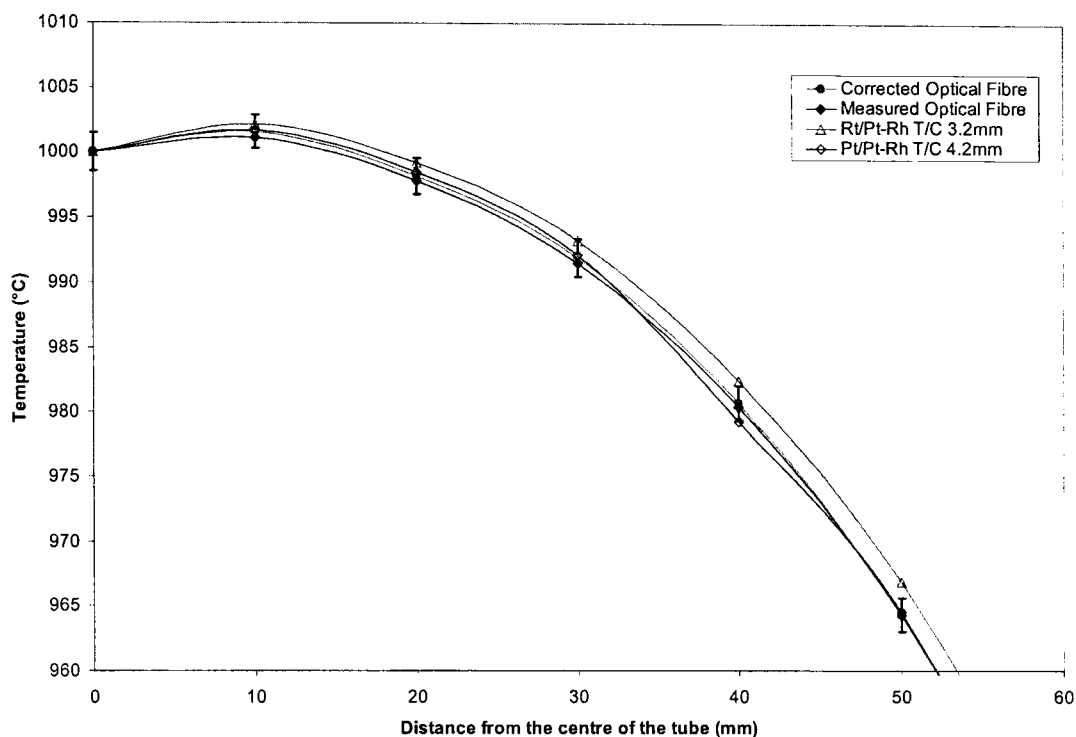


Figure 7. Plot of the optical fibre measured and corrected results with their uncertainty bars compared with the measurements taken by Pt/Pt-Rh thermocouple wires in alumina tubes with 3.2 and 4.2 mm diameter within 50 mm of the graphite tube centre.

[4] ISO Guide to the Expression of Uncertainty in Measurement, 1994.

7. Conclusions

A simple method for measuring the surface temperature of a tube furnace by correcting measurements from an optical fibre for reflections has been developed. We have obtained satisfactory agreement between thermocouple and reflection-corrected optical fibre measurements, confirming that both methods are suitable for measuring the gradients in the tube furnace.

8. References

- [1] Ballico, M. (2000). "Simple technique for measuring the infrared emissivity of black-body radiators." *Metrologia* 37(4): 295-300.
- [2] Ballico, M. (1998). *Radiation Thermometry. Temperature and Humidity Measurement*. R. E. Bentley. Singapore, Springer-Verlag. 1: 67-97.
- [3] Siegel, R. and J. R. Howell (2002). *Thermal radiation heat transfer*. London, Taylor & Francis.